Phys. Status Solidi A **211**, No. 11, 2475–2482 (2014) / **DOI** 10.1002/pssa.201431195

physica status solidi a
www.pss-a.com
applications and materials science

Atomic-layer-deposited zinc oxide as tunable uncooled infrared microbolometer material

Enes Battal[1], Sami Bolat[1], M. Yusuf Tanrikulu[*,3], Ali Kemal Okyay[2], and Tayfun Akin[4]

[1] Department of Electrical and Electronics Engineering, UNAM – National Nanotechnology Research Center, Bilkent University, Ankara 06800, Turkey
[2] Department of Electrical and Electronics Engineering, Institute of Materials Science and Nanotechnology, UNAM – National Nanotechnology Research Center, Bilkent University, Ankara 06800, Turkey
[3] Department of Electrical-Electronics Engineering, Adana Science and Technology University, Adana 01180, Turkey
[4] Department of Electrical and Electronics Engineering, METU MEMS – Micro Electro Mechanical Systems Center, Middle East Technical University, Ankara 06531, Turkey

Received 19 March 2014, revised 30 May 2014, accepted 31 May 2014
Published online 7 July 2014

Keywords atomic layer deposition, bolometers, electrical conduction, semiconductors, thin films, ZnO

* Corresponding author: e-mail mytanrikulu@adanabtu.edu.tr, Phone: +90 322 455 00 00/2059, Fax: +90 322 455 00 09

ZnO is an attractive material for both electrical and optical applications due to its wide bandgap of 3.37 eV and tunable electrical properties. Here, we investigate the application potential of atomic-layer-deposited ZnO in uncooled microbolometers. The temperature coefficient of resistance is observed to be as high as $-10.4\%\,K^{-1}$ near room temperature with the ZnO thin film grown at 120 °C. Spectral noise characteristics of thin films grown at various temperatures are also investigated and show that the 120 °C grown ZnO has a corner frequency of 2 kHz. With its high TCR value and low electrical noise, atomic-layer-deposited (ALD) ZnO at 120 °C is shown to possess a great potential to be used as the active layer of uncooled microbolometers. The optical properties of the ALD-grown ZnO films in the infrared region are demonstrated to be tunable with growth temperature from near transparent to a strong absorber. We also show that ALD-grown ZnO can outperform commercially standard absorber materials and appears promising as a new structural material for microbolometer-based applications.

© 2014 WILEY-VCH Verlag GmbH & Co. KGaA, Weinheim

1 Introduction ZnO has found a broad range of applications in thin-film electronics, sensors, and optoelectronics due to its remarkable electronic and optical properties [1, 2]. Owing to its wide bandgap of 3.37 eV and high defect-related electrical conductivity, ZnO has long been used as transparent and conducting coatings [3, 4]. The high electron mobility of ZnO, makes it a very suitable material for thin-film transistors in display applications, emerging as a strong rival to amorphous silicon [5, 6]. ZnO has also been investigated for ultraviolet sensing applications due to its band edge at 367 nm [7], however, its infrared properties, especially for imaging applications, have not been exploited.

Microbolometers are the most preferred infrared imagers and have significant advantages compared to cooled detectors such as room-temperature operation, low cost, compactness, high durability, CMOS compatibility, and low weight. In microbolometers, typically, a pixel body consists of an infrared-absorbing layer, a thermally sensitive active layer, and a structural material for mechanical support. The resistance of the active layer changes upon heating of the pixel body by absorbed infrared radiation. The change in pixel resistance is detected via standard CMOS read-out circuitry [8]. Commercial-grade bolometers employ Si_3N_4 as both the structural and the infrared-absorbing layer [8]. The gold standard among thermally sensitive materials are vanadium oxide (VO_x) and amorphous silicon (a-Si), with temperature coefficient of resistance (TCR) values reaching up to -4 and $-2.5\%\,K^{-1}$, respectively [9–11].

Recently, there is a tremendous effort towards finding alternatives to currently used standard materials in order to push the performance limits of microbolometer devices further. Materials with stronger absorption in the infrared are sought after to increase the responsivity of bolometers [12–14] and/or to reduce the film thicknesses in order to achieve smaller thermal time constants, hence faster

© 2014 WILEY-VCH Verlag GmbH & Co. KGaA, Weinheim

operation. Materials with higher TCR values can increase the efficiency of the bolometers and provide lower noise equivalent temperature difference (NETD) performance [15–17].

ZnO has attracted attention to be used as the active layer of the microbolometer detectors, due to its potential to have TCR values higher than that of the commercially used materials. Several research groups have obtained results suggesting that ZnO indeed has higher TCR values than VO_x and a-Si [18]. In the reported works, ZnO films have been deposited using various methods such as pulsed laser deposition (PLD) [18], and sputtering [19]. Zhou et al. used PLD technique for ZnO deposition, and they observed TCR values ranging from -3.4 to $-13\%\,K^{-1}$ [18]. However, these values were measured at temperatures much lower than room temperature. Liu et al. have studied the effects of annealing ZnO/p-Si heterojunctions, on the TCR values of grain boundaries [19]. In their work, they have shown that the annealing of the sputter deposited ZnO on p-Si substrate in a N_2 environment at 800 °C results in positive TCR values, whereas as-deposited layers and the layers annealed in an O_2 environment at 800 °C exhibit negative TCR values. He et al. have observed positive TCR values in the 383–473 K temperature range with ZnO nanorods, which have been synthesized using an aqueous solution method [20].

In addition to its potentially high TCR value, the optical properties of ZnO are also important for simultaneous use as both an infrared-absorbing layer and a thermally sensitive layer in microbolometers. Surprisingly, there are very limited reports on the infrared (IR) properties and applications of ZnO in the literature. Especially for IR imaging applications, precise knowledge of dielectric optical properties of ZnO is crucial. In the IR spectrum, free carriers are well known to modulate optical properties in contrast to phonon modes that arise due to crystal structure of materials. Phonon modes of ZnO thin films grown by the PLD technique have been shown to be very effective in defining the optical constants in the 300–600 cm^{-1} (~16–33 μm) range [21]. However, investigation of IR optical properties of ZnO thin films grown by the ALD technique, which is known to provide good control over the free-carrier concentration [22], still remains to be explored. Atomic-layer deposition is a promising deposition technique, because of its high uniformity, conformity, and precise control of the thickness of the grown film, even at low temperatures [23]. Up to now, there are no reported works on the use of the ALD-grown ZnO as IR absorbing or thermally sensitive material for microbolometer applications. In this paper, we investigate, for the first time, the TCR and electrical noise together with the optical properties of ALD-grown ZnO and discuss its suitability for thermal IR sensing applications. A TCR of $-10.4\%\,K^{-1}$, which is particularly higher than that of commercially used bolometer materials, has been obtained with ZnO grown at 120 °C. This material is also shown to have a corner frequency of 2 kHz in the spectral noise power density spectrum. With variation of the growth temperature, the optical properties of the films are shown to vary greatly and an absorbing structure better than a commercially standard material is achieved.

2 Electrical measurements

TCR, which represents the normalized change in the resistance with respect to temperature, is calculated by using the following formula:

$$\mathrm{TCR} = \frac{1}{R} \times \frac{\mathrm{d}R}{\mathrm{d}T}, \tag{1}$$

where R represents the resistance of the thin film, and T represents the temperature. Figure 1 shows the temperature-dependent resistance and TCR characteristics of the ZnO thin films grown at 120 °C. The results indicate that the TCR of the grown films strongly depends on measurement

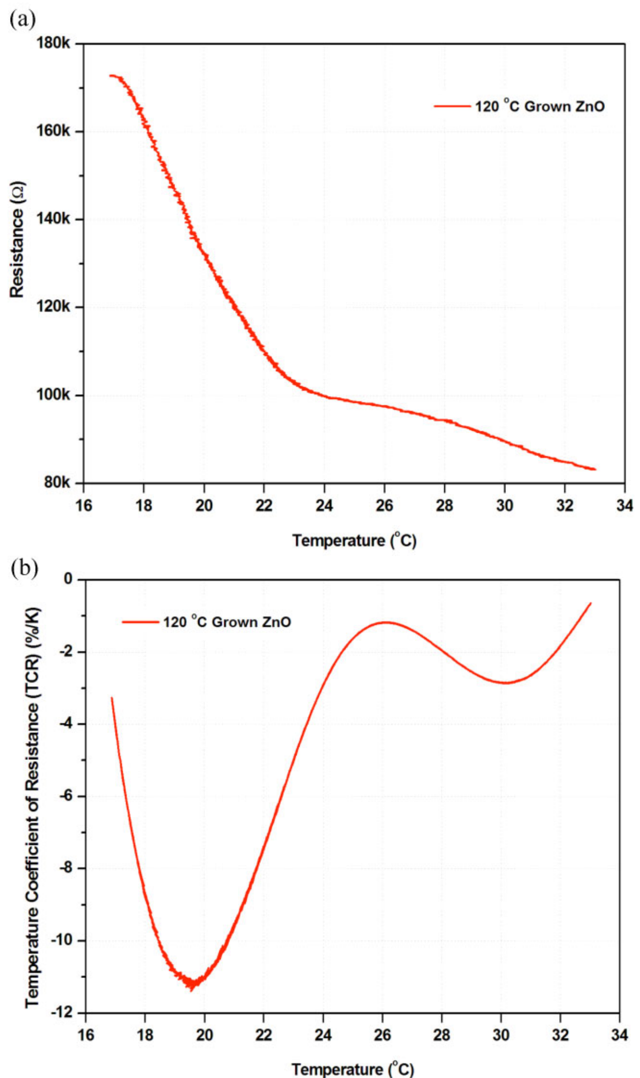

Figure 1 Temperature-dependent resistance and TCR characteristics of ZnO thin films grown at 120 °C. ZnO films possess TCR values up to $-10.4\%\,K^{-1}$ near room temperature, which is higher than the commercial alternatives. Films grown at 200 and 250 °C exhibit very low TCR ($<1\%\,K^{-1}$) in the measurement range.

© 2014 WILEY-VCH Verlag GmbH & Co. KGaA, Weinheim

Table 1 Resistivity and maximum TCR values the ZnO films grown at different temperatures.

growth temperature (°C)	maximum TCR ($\% \mathrm{K}^{-1}$)	temperature at which TCR is maximum (°C)	resistivity ($\Omega\,\mathrm{cm}^{-1}$)
120	−10.4	20	13.5–100
200	−0.05	16	0.015
250	0.07	16	0.009

temperatures and 120 °C grown ZnO films possess TCR values up to $-10.4\% \mathrm{K}^{-1}$ near room temperature.

For the films grown at 200 and 250 °C, TCR values are near zero, which is generally observed in films with high conductivities. Table 1 shows the maximum TCR of the ZnO thin films grown at different temperature levels, and the temperature level at which the maximum TCR has been obtained.

The TCR of ZnO thin film grown at 250 °C is positive, whereas the TCR values of the films grown at lower temperatures are negative. This suggests that the behavior of a 250 °C grown film is similar to that of conductors, whereas the ZnO thin films grown at lower temperatures have the typical behavior of semiconducting materials. This is consistent with the reported resistivity values of ALD-grown ZnO films in the literature [24].

Table 1 also shows the resistivity of the ZnO thin films grown at different temperatures. Increasing deposition temperature results in higher free-carrier concentrations, therefore, lower resistivity values. This behavior is in agreement with earlier reports on ZnO deposited by ALD and sputtering in similar deposition temperature ranges [24]. ZnO films exhibit n-type behavior, where n-type conductivity is generally attributed to the existence of the zinc interstitials, and oxygen vacancies [25]. The decrease of resistance with increasing deposition temperature indicates that the ZnO grown at higher temperatures has a Zn-rich composition, whereas the ZnO films grown at lower temperature levels are oxygen-rich, as previously reported [25]. These results also support the change of sign (from negative to positive) in measured TCR values of ZnO grown at higher temperatures, suggesting that ZnO deposited at 250 °C behaves as a decent conductor, but a semiconductor when deposited at 120 °C.

Active layers with low electrical noise are sought in order to achieve high sensitivity and detectivity in microbolometers. Important components of the electrical noise in microbolometers are mainly flicker noise and thermal noise. The spectral noise analyses of the grown films have been performed on resistors patterned on such films. Figure 2 shows the noise power spectral densities (NPSD) of the thin-film ZnO resistors grown at 120, 200, and 250 °C.

A logarithmic NPSD–frequency plot indicates that flicker noise is the dominant mechanism in the 200 and 250 °C grown ZnO thin films within the measured frequency range (0–10 kHz). The corner frequency of 120 °C grown ZnO is at about 2 kHz, which falls in the suitable range for the bolometers operating in snapshot mode [26]. The obtained results suggest that the ZnO thin film grown at 120 °C with the ALD method, in terms of electrical properties, is a very promising candidate to be used as the active layer of uncooled microbolometers.

3 Optical measurements Investigation of the optical properties of ZnO films is crucial for ALD-grown ZnO to be a candidate for structural or active material for IR microbolometers. The optical properties of the films are described by their complex refractive indices, $\tilde{n} = \sqrt{\varepsilon} = n + jk$, where ε is the permittivity and n and k are the real and the imaginary parts, respectively. In order to determine the complex refractive indices of the films, a spectroscopic ellipsometry technique is used. In this method, the change in the polarization of the reflected light

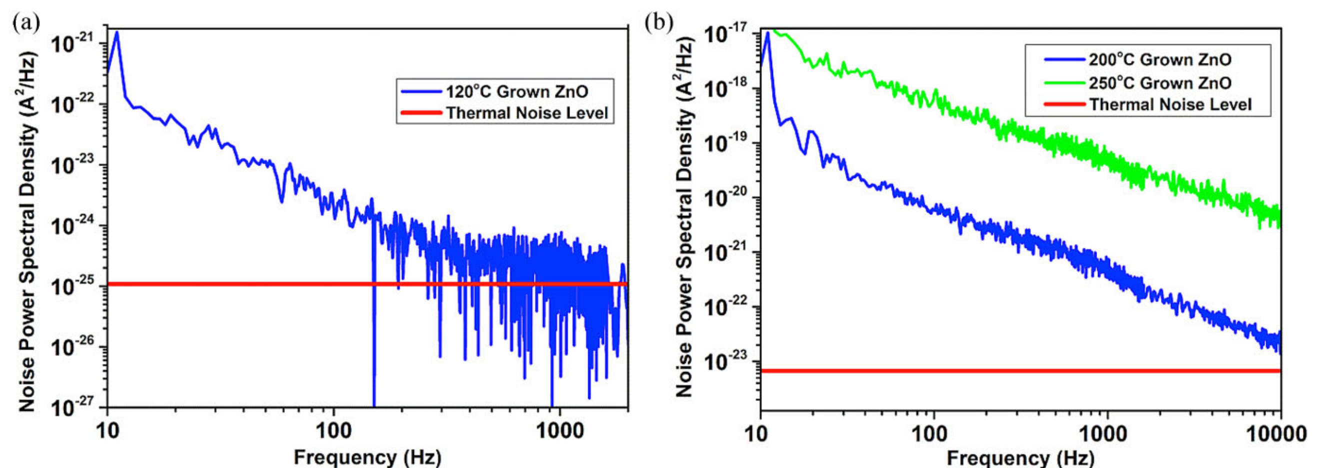

Figure 2 Noise power spectral densities of the thin film ZnO resistors grown at (a) 120 °C, (b) 200 °C and 250 °C show that the ZnO grown at 120 °C has a corner frequency of 2 kHz, whereas the corner frequencies of the thin films deposited at higher measurements are not observed within the measurement range.

© 2014 WILEY-VCH Verlag GmbH & Co. KGaA, Weinheim

Table 2 Cauchy dispersion model fit parameters with respect to ZnO growth temperature for the 400–1700 nm region where ZnO films are transparent.

growth temperature (°C)	thickness (nm)	A	B	C	A_k	E_k (eV)
80	38.5	1.818	4.37×10^{-2}	4.13×10^{-4}	4.55×10^{-2}	1.73
120	45.5	1.816	5.05×10^{-2}	3.92×10^{-4}	4.68×10^{-2}	1
200	44.9	1.813	4.74×10^{-2}	2.84×10^{-4}	2.82×10^{-2}	0.2
250	34.6	1.786	3.03×10^{-2}	2.84×10^{-3}	2.18×10^{-2}	0.229

represented by the complex reflectance ratio,

$$\rho = \frac{r_p}{r_s} = \tan(\Psi)e^{j\Delta}, \tag{2}$$

is determined by measuring Ψ and Δ that are amplitude ratio and phase shift. Then, these parameters are converted to the Fresnel reflection coefficients for p-polarized (r_p) and s-polarized (r_s) light and fit using dispersive dielectric function models.

ZnO films exhibit transparency starting from the bandgap of ZnO and reaching up to near-IR wavelengths. Therefore, the Cauchy dispersion model, which is well known to characterize transparent thin films [27], is used in the 400–1700 nm region to precisely determine the thickness of the films. Cauchy dispersion parameters are defined with the following formula:

$$n(\lambda) = A + \frac{B}{\lambda^2} + \frac{C}{\lambda^4}, \tag{3}$$

$$k(\lambda) = A_k e^{E_k((\hbar c/\lambda)E_b)},$$

where A, B, C, A_k, and E_k are fit parameters for the model and E_b is the band edge, which is assumed to be 3.37 eV. Table 2 lists the parameters resulting in the best fit.

In the IR region, the effect of free carriers should be taken into account using the Drude oscillator model as IR spectroscopic ellipsometry provides access to the free carriers and the grown films are measured to have a considerable number of free carriers. In the spectral range of interest, 1.8–15 μm, the dielectric permittivities of the films are modeled using a Drude oscillator combined with a Lorentz oscillator with the following formulation,

$$\varepsilon(\omega) = \varepsilon'(\omega) + j\varepsilon''(\omega) = \varepsilon_\infty + \varepsilon_{\mathrm{Drude}}(\omega) + \varepsilon_{\mathrm{Lorentz}}(\omega),$$

$$\varepsilon_{\mathrm{Drude}}(\omega) = -A\frac{\Gamma}{((\hbar\omega)^2 + j\Gamma\hbar\omega)},$$

$$\varepsilon_{\mathrm{Lorentz}}(\omega) = A\frac{\Gamma\hbar\omega_n}{(\hbar\omega_n)^2 - (\hbar\omega)^2 - j\Gamma\hbar\omega},$$

where $\hbar$ is Planck's constant, ε_∞ is the static dielectric permittivity, A is the amplitude of the oscillator, Γ is the broadening, ω_n is the center frequency of the oscillator, and ω is the frequency.

Using the determined thickness values in Table 2 and assuming isotropic films, a nonlinear least square error algorithm is employed to fit IR dielectric functions. As the resistivity of the 80 °C samples is considerably high, the free-carrier effects were not apparent; therefore, Drude oscillator parameters are not used for this growth temperature. Table 3 shows the parameters resulting in the best fit and Fig. 3 depicts the extracted real and imaginary parts of the permittivity as a function of growth temperature. By varying the growth temperature, the fit parameters show significant change in the Drude oscillator parameters due to modulation of free-carrier properties, whereas Lorentz oscillator model parameters are quite invariant. Such invariance of Lorentz oscillator parameters is attributed to be correlated with phonon mode properties of the films, which are not expected to significantly modulate the spectrum of interest by growth-temperature variations.

For control purposes, reflection measurements from ZnO films are performed using a bare Si wafer as the reference. Figure 4 compares the measured reflection measurements with from ZnO-coated Si samples with the simulated reflection values generated using the extracted optical constants. Very good agreement between the measurements and the simulations is obtained.

The imaginary part of the permittivity (ε'') is an indicator of the absorption characteristics of the films. The films get highly absorptive with increasing growth temperature as ε'' increases significantly. Since highly absorbing films are

Table 3 Fit parameters for the infrared region as a function of ZnO growth temperature.

growth temperature (°C)	ε_∞	Lorentz			Drude	
		A	Γ (cm^{-1})	ω_n (cm^{-1})	A (cm^{-1})	Γ (cm^{-1})
80	3.70	35.7	47.07	396.5	–	–
120	3.71	51.2	48.3	397.3	1694	8468
200	3.65	51.6	52.74	397	8109	2024
250	3.25	55.8	60.98	396.5	14 886	2241

© 2014 WILEY-VCH Verlag GmbH & Co. KGaA, Weinheim

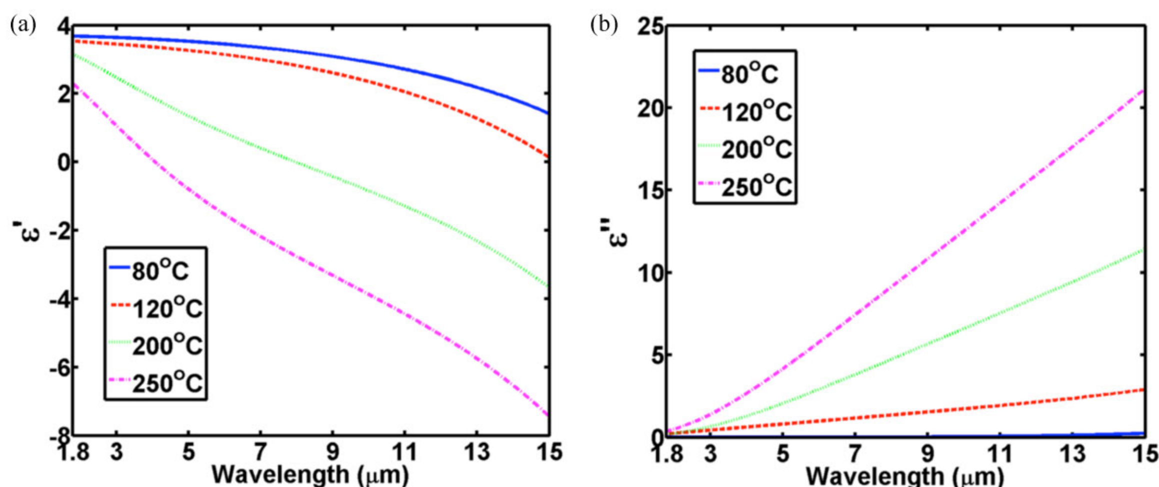

Figure 3 (a) Real (ε′) and (b) imaginary (ε″) parts of the permittivities of the grown ZnO films with respect to growth temperature indicate an increasing metallic behavior with increasing growth temperature, as a result of the rise in the free-carrier concentration.

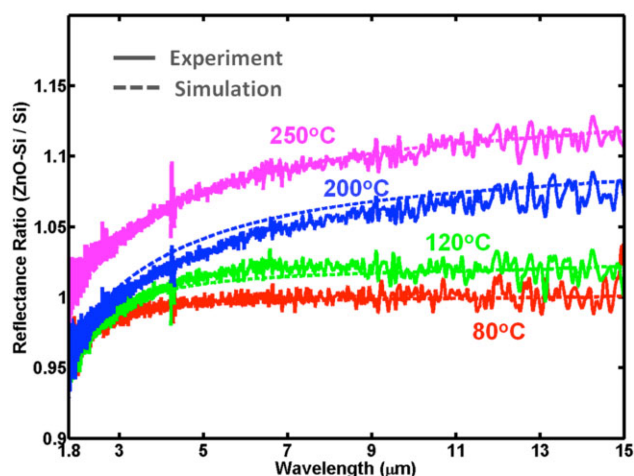

Figure 4 FTIR reflection measurements (solid) and simulations (dashed) using the extracted values yield a very good agreement. Increased reflectance with the increasing growth temperature indicates a better metallic behavior for ZnO films grown at higher temperatures.

sought after for IR bolometric applications, such high absorption performance and controllability makes ALD-grown ZnO a potentially very attractive candidate. To exemplify the absorption performance of the films, a theoretical comparison between a reference bolometer structure [28] with a commercially standardized material structural material, Si_3N_4, and the grown films is carried out using FDTD simulations. Figure 5a shows the simulated reference structure, a 400-nm thick suspended absorber layer having an air gap of 2 μm above a metallic reflector, using the optical constants of the ZnO films and Si_3N_4 [28]. Figure 5b depicts the simulated absorption spectra of the films. All ZnO films exhibit a significant amount of absorption in the bolometric region of interest, 8–12 μm. In addition, 200 and 250 °C grown ZnO films also show considerable amount of absorption in the 3–5 μm region, which is also exploited for bolometric IR imaging purposes. Figure 5c compares integrated absorption in 8–12 μm for Si_3N_4 and the ZnO films. In this spectrum, all ZnO films except 80 °C grown film exhibit absorptivity values comparable to that of Si_3N_4. 200 °C grown ZnO shows 85% absorption, which outperforms Si_3N_4 by 13%. Considering the resulting stress-free characteristics along with the remarkable optical performance (see Supporting Information, online at www.pss-a.com), ZnO films grown at 200 °C appears as a very attractive structural material for bolometric applications. The relatively lower absorption of 80 °C grown ZnO films is attributed to the fact that ε″ is well below 1 in the entire spectrum. Yet, this material can still be useful as a low-loss broadband IR antireflective coating layer as its refractive index varies between 1.45 and 1.9.

Modulation of growth temperature also provides control over the real part of the permittivity (ε′). The wavelength at which the real part of the permittivity equals zero is defined as the plasma wavelength (λ_p) of the material. Above this wavelength, the material exhibits similar optical characteristics to that of a metal due to free carriers. The λ_p value of the films redshifts with decreasing growth temperatures, which is an indication of the decreasing carrier conductivity as observed in the electrical measurements. Although 120 and 80 °C grown samples have a considerable number of free carriers with concentrations on the order of 1×10^{16} and $1 \times 10^{17}\,cm^{-3}$, respectively, their λ_p do not fall into the region of investigation. However, the trend of the real part of the permittivity indicates that the λ_p of 120 °C is lower than that of 80 °C due to the higher carrier concentration at 120 °C. For 200 and 250 °C growth temperatures, λ_p is determined to be about 8 and 4.08 μm, respectively. The increasing reflectivity from the samples with the increasing growth temperature indicates that the highly conductive

 © 2014 WILEY-VCH Verlag GmbH & Co. KGaA, Weinheim

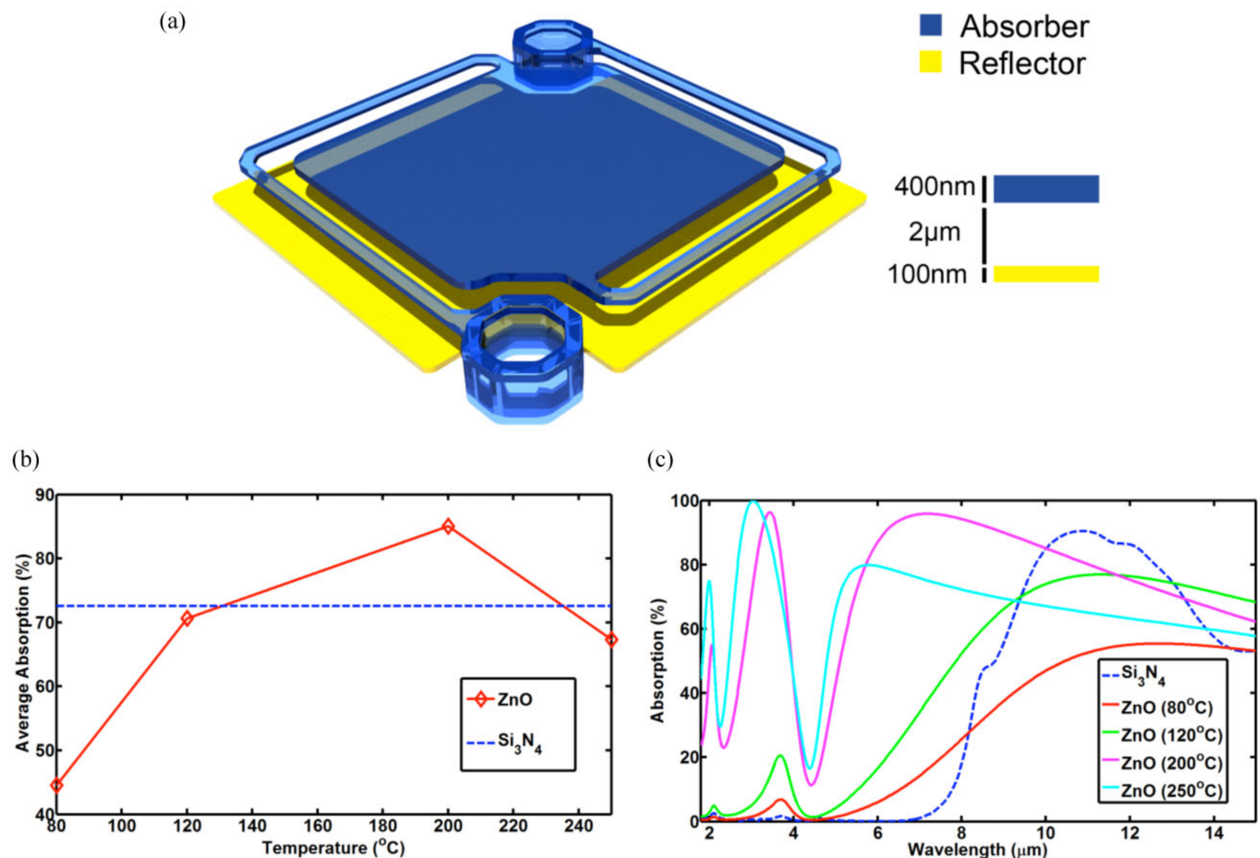

Figure 5 (a) 3D view of the simulated standard bolometer structure. (b) Simulation results of average absorption of ZnO films in the 8–12 μm region indicates a higher performance for 200 °C grown films compared to Si_3N_4. Broadband absorption characteristics is observed in (c) the absorption spectra of the films including a significant amount of absorption in the 3–5 μm region, as well.

films are closer to the metallic behavior optically. Such metallic behavior sets the scene for exploiting dielectric-based metal-optics in bolometric applications.

4 Conclusion In conclusion, we have investigated the TCR and electrical noise together with the optical properties of the ALD-grown ZnO for the first time for its usage in uncooled microbolometers. Depositions are performed at various temperatures to observe the effect of the growth temperature on the properties of the ZnO. In terms of electrical properties, a tendency of becoming more conductive with the increase in the deposition temperature has been observed and it is related to the defect-rich structure of the deposited thin film. The optical constants of the films are modeled using the Drude and Lorentz oscillator models. The optical properties of the films can be tailored thanks to the flexibility on controlling the free-carrier concentrations of the films by varying growth temperature in the ALD process. By increasing the growth temperature, the films turn from a poorly absorbing semiconductor to a strongly absorbing highly conductive material. Compared to a standard layer, 200 °C grown films exhibit greater absorption in a typical bolometer structure. Owing to several advantageous properties obtained by only changing the deposition temperature, ALD-grown ZnO has a great potential for its usage in uncooled microbolometers. 120 °C grown ZnO with the TCR of $-10.4\%\ K^{-1}$ and flicker noise corner frequency of 2 kHz is a promising candidate on replacing the currently used active layer materials of commercial microbolometers, whereas 200 °C grown ZnO with its broad band and high absorption characteristics is a great candidate to replace Si_3N_4 as the structural and absorbing material of uncooled microbolometers.

A Experimental procedure

A.1 Electrical characterization Electrical characteristics of ZnO films grown with the ALD technique are investigated. The ALD process is performed in a Cambridge Savannah 100 Thermal ALD system using diethylzinc (DEZ) and milli-Q water (H_2O) as reaction precursors. In order to observe the effects of growth temperature, the films are deposited at temperatures of 80, 120, 200, and 250 °C. All substrates are cleaned with a standard RCA cleaning process.

Van der Pauw structures are used for resistivity characterization. For flicker noise and TCR measurements,

© 2014 WILEY-VCH Verlag GmbH & Co. KGaA, Weinheim

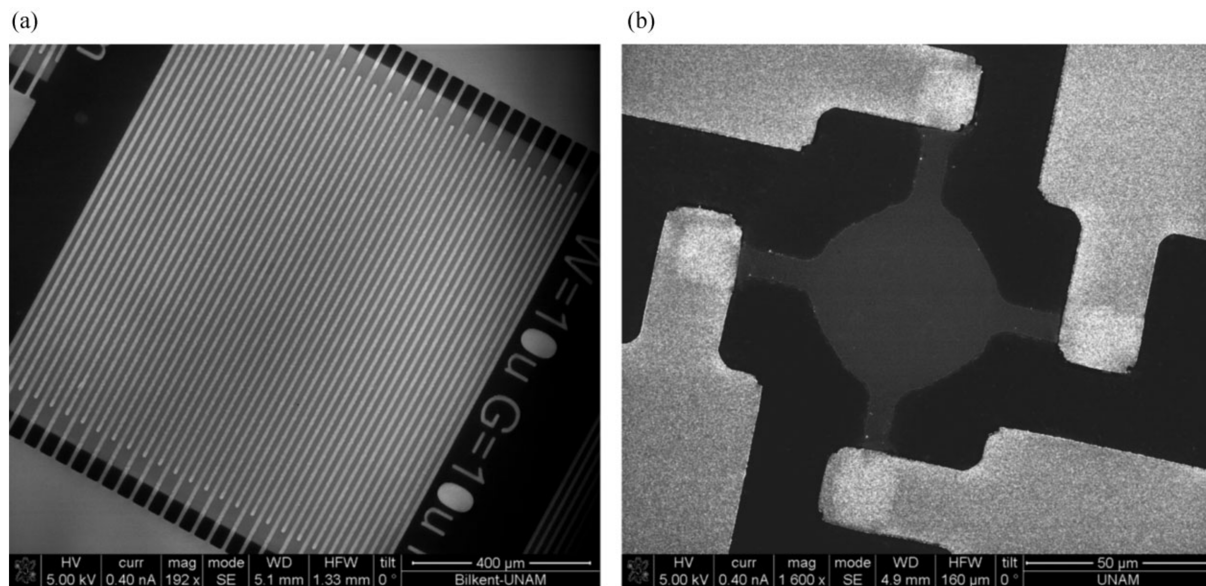

Figure 6 Noise and TCR measurements are carried out with (a) interdigitated finger structures, and resistivity measurements are performed on Van der Pauw structures (b).

interdigitated finger structures are used. Fabrication of structures are performed using standard optical lithography, BCl_3-based dry etching of ZnO and thermal evaporation of metal contacts. SEM images of completed interdigitated and Van der Pauw structures are shown in Fig. 6a and b, respectively. Noise measurements are performed using an analog amplifier integrated with a spectrum analyzer at room temperature. A temperature-controlled environment is used for TCR measurements. The environment temperature is increased from 15 to 35 °C in a period of 30 min, while voltages across the resistors are recorded under constant current bias.

A.2 Optical characterization Ellipsometric optical characterization is carried out on 300-cycles-thick ZnO film grown on n-type (100) Si wafers with a resistivity of 3–5 kΩ cm. For short (0.4–1.7 µm) and long (1.8–15 µm) wavelengths, commercial spectroscopic ellipsometers, V-Vase and IR-Vase from J.A. Woollam Inc. are used, respectively. The ellipsometric data is collected at incidence angles of both 57° and 67° to minimize fit errors. Using a Fourier transform infrared (FTIR) Spectrometer (Bruker Vertex 70 and Hyperion 2000), reflection measurements are performed on the same samples in order to verify the extracted optical properties.

Acknowledgements This work was supported by the Scientific and Technological Research Council of Turkey (TUBITAK), grant numbers 109E044, 112M004, 112E052, 113M815, and 113M912, FP7 Marie Curie IRG grant 239444. A. K. O. acknowledges a Marie Curie International Reintegration Grant (IRG). E. B and S. B. are supported by TUBITAK-BIDEB MS fellowships.

References

[1] G. D. Yuan, W. J. Zhang, J. S. Jie, X. Fan, J. X. Tang, I. Shafiq, Z. Z. Ye, C. S. Lee, and S. T. Lee, Adv. Mater. **20**, 168 (2008).
[2] U. Ozgur, Y. I. Alivov, C. Liu, A. Teke, M. A. Reshchikov, S. Dogan, V. Avrutin, S.-J. Cho, and H. Morkoc, J. Appl. Phys. **98**, 041301 (2005).
[3] E. Klaus, J. Phys. D, Appl. Phys. **33**, R17 (2000).
[4] A. Yamada, B. Sang, and M. Konagai, Appl. Surf. Sci. **112**, 216 (1997).
[5] E. M. C. Fortunato, P. M. C. Barquinha, A. C. M. B. G. Pimentel, A. M. F. Gonçalves, A. J. S. Marques, L. M. N. Pereira, and R. F. P. Martins, Adv. Mater. **17**, 590 (2005).
[6] R. L. Hoffman, B. J. Norris, and J. F. Wager, Appl. Phys. Lett. **82**, 733 (2003).
[7] Z. K. Tang, G. K. L. Wong, P. Yu, M. Kawasaki, A. Ohtomo, H. Koinuma, and Y. Segawa, Appl. Phys. Lett. **72**, 3270 (1998).
[8] A. Rogalski, Infrared Phys. Technol. **43**, 187 (2002).
[9] C. Chen, X. Yi, J. Zhang, and X. Zhao, Infrared Phys. Technol. **42**, 87 (2001).
[10] E. Mottin, J.-L. Martin, J.-L. Ouvrier-Buffet, M. Vilain, A. Bain, J.-J. Yon, J.-L. Tissot, and J.-P. Chatard, Proc. SPIE **4369**, 250 (2001).
[11] Y. Ningyi, L. Jinhua, H. L. W. Chan, and L. Chenglu, Appl. Phys. A **78**, 777 (2004).
[12] C. M. Watts, X. Liu, and W. J. Padilla, Adv. Mater. **24**, OP98 (2012).
[13] Z. H. Jiang, S. Yun, F. Toor, D. H. Werner, and T. S. Mayer, ACS Nano **5**, 4641 (2011).
[14] T. Asano, H. Chong, Z. Yi, L. Mingguo, J. C. Campbell, and A. Madhukar, IEEE J. Quantum Electron. **46**, 1484 (2010).
[15] F. B. Atar, A. Yesilyurt, M. C. Onbasli, O. Hanoglu, and A. K. Okyay, IEEE Electron Device Lett. **32**, 1567 (2011).

© 2014 WILEY-VCH Verlag GmbH & Co. KGaA, Weinheim

[16] J. Yan, M. H. Kim, J. A. Elle, A. B. Sushkov, G. S. Jenkins, H. M. Milchberg, M. S. Fuhrer, and H. D. Drew, Nature Nanotechnol. **7**, 472 (2012).
[17] A. Y. Glamazda, V. A. Karachevtsev, W. B. Euler, and I. A. Levitsky, Adv. Funct. Mater. **22**, 2177 (2012).
[18] X.-F. Zhou, H. Zhang, Y. Li, X.-D. Tang, Q.-M. Chen, and P.-X. Zhang, Chin. Phys. Lett. **27**, 018101 (2010).
[19] B. Liu, C. Liu, J. Xu, and B. Yi, J. Semicond. **31**, 122001 (2010).
[20] G. He, H. Bo, and S. Hui, Nanotechnology **22**, 065304 (2011).
[21] S. Heitsch, C. Bundesmann, G. Wagner, G. Zimmermann, A. Rahm, H. Hochmuth, G. Benndorf, H. Schmidt, M. Schubert, M. Lorenz, and M. Grundmann, Thin Solid Films **496**, 234 (2006).
[22] S. J. Lim, S.-J. Kwon, H. Kim, and J.-S. Park, Appl. Phys. Lett. **91**, 183517 (2007).
[23] M. Ritala and J. Niinisto, Atomic Layer Deposition, in: Chemical Vapour Deposition: Precursors, Processes and Applications (The Royal Society of Chemistry, UK, 2009), p. 158, doi: 10.1039/9781847558794-00158.
[24] S. J. Lim, S. Kwon, and H. Kim, Thin Solid Films **516**, 1523 (2008).
[25] E. Guziewicz, M. Godlewski, L. Wachnicki, T. A. Krajewski, G. Luka, S. Gieraltowska, R. Jakiela, A. Stonert, W. Lisowski, M. Krawczyk, J. W. Sobczak, and A. Jablonski, Semicond. Sci. Technol. **27**, 074011 (2012).
[26] A. Rogalski, Prog. Quantum Electron. **27**, 59 (2003).
[27] Y. C. Liu, J. H. Hsieh, and S. K. Tung, Thin Solid Films **510**, 32 (2006).
[28] O. Erturk, E. Battal, S. E. Kucuk, A. K. Okyay, and T. Akin, Proc. SPIE **8704**, 87041E (2013).

Supporting Information

Additional Supporting Information may be found in the online version of this article at the publisher's website.

© 2014 WILEY-VCH Verlag GmbH & Co. KGaA, Weinheim